Molecular dynamics modeling of unsaturated clay-water systems at elevated temperature

X. Song & M. Wang

Department of Civil and Coastal Engineering, University of Florida, Florida, USA

K. Zhang

Department of Computer Science, Carnegie Mellon University, Pennsylvania, USA

ABSTRACT: The hydromechanical behavior of unsaturated clay under non-isothermal conditions has practical implications in geotechnical engineering (e.g., geothermal energy). The water menisci among clay particles impact the hydromechanical behavior of unsaturated clay. In this paper, we investigate the impact of temperature variation on the unsaturated clay-water system via a full-scale molecular dynamics (MD) modeling. The water meniscus formed between two clay platelet particles is simulated via the classical MD modeling at elevated temperatures. We report the impact of temperature on the capillary force and the meniscus topology. By providing physical interfacial properties of unsaturated clay at the atomic scale directly from the numerical simulation, the MD simulation of unsaturated clay-water systems has a significant implication in formulating a physical based multiscale modeling technique for unsaturated soils from the atomic scale to continuum scale.

1 INTRODUCTION

Unsaturated soils play a significant role in geotechnical and geoenvironmental engineering (Fredlund & Rahardjo 1993, Lu & Likos 2004, Ng & Menzies 2007). However, our knowledge of the fundamental failure mechanism of unsaturated soils under the environmental loads (e.g., humidity and temperature) is limited (Borja et al. 2014, Song & Borja 2014, Song 2017, Song et al. 2017, Song et al. 2018). The physical behavior of clay is controlled at the particle level by the van der Waals, double-layer due to electrostatic interactions, and capillary interactions (Mitchell & Soga 2005). The capillary phenomena among soil grains, water, and air have a profound impact on the mechanical and transport properties of unsaturated soils. To examine the capillarity, we need to understand the capillary forces, contact angles, and meniscus curvatures. Clay and its related phases present a particularly daunting set of challenges for the experimentalist and computational chemist (Teppen et al. 1995, Cygan et al. 2004, Amarasinghe et al. 2014). For this reason, molecular dynamics simulations on supercomputers have become extremely helpful in providing an atomic perspective on the structure and behavior of clay minerals. Temperature variation influences both mechanical and physical properties of unsaturated clay (Mitchell & Soga 2005, Ng & Menzies 2007). In this paper, we study the temperature

impact on the capillary force on the clay particle imposed by water meniscus via a full-scale MD modeling. In this study, we output the capillary force of an unsaturated clay-water system directly from the MD simulation. The preliminary results demonstrate that MD simulations can be utilized to characterize the temperature impact on the capillary force as well as the variation of meniscus curvatures of unsaturated clay at the atomic scale. The finding has practical implications in formulating physical-based multi-scale models for unsaturated soils which bridges the atomic scale and the continuum scale.

2 METHODS AND MATERIALS

2.1 Molecular dynamics

Molecular dynamics is a useful computational method for studying physical and chemical phenomena occurring at the atomic scale. MD simulation is a technique for computing the equilibrium and transport properties of a classical many-body system (Frenkel & Smit 2002). In MD, the positions, velocities, and accelerations of the atoms in a molecular system are computed by numerically solving the equations of Newton's second law of motion (Plimpton 1995). Energy of the molecular system is expressed using suitable empirical potential energy functions or force fields (Cygan et al. 2004, Brook et

al. 1983). Successful application of any computational molecular modeling technique requires the use of interatomic potentials (force fields) that effectively and accurately account for the interactions of all atoms in the model system.

2.2 Unit cell

The clay in this study is pyrophyllite, a 2:1 smectite mineral, consisting of an octahedral sheet sandwiched between two silica sheets, whose chemical formula is Al₂Si₄O₁₀(OH)₂ (Mitchell & Soga 2005). Figure 1 (a) shows the molecular structure of a unit cell of pyrophyllite. The dimension of a unit cell in the x-y-z Cartesian coordinate system is 5.2 Å x 9.14 Å x 6.56 Å (1 $Å = 10^{-10} \text{ m} = 0.1 \text{ nm}$) which consists of 40 atoms (Skipper et al. 1995). In this study, the rigid TIP3p water model (Jorgensen et al. 1983) is used to generate a water body between two clay platelet particles. Figure 1 (b) shows the molecular structure of water. In this paper, we consider a water body sandwiched between two parallel clay particles which is a typical structure of platelet clay minerals (Mitchell & Soga 2005).

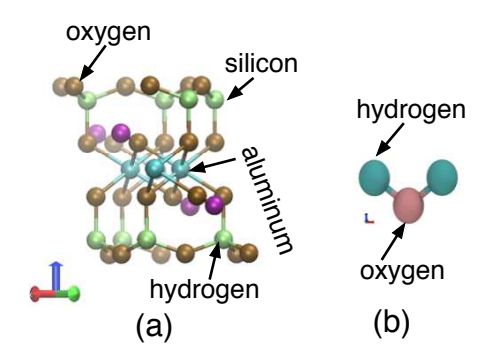


Figure 1. (a) Molecular structure of a unit cell of pyrophyllite; (b) Molecular structure of water.

2.3 Clay-water system

In this study, the non-bonded potential energy for clay is represented by a CHARMM force field casted for pyrophyllite (Teppen et al. 1997, Katti et al. 2005). A CHARMM potential for the TIP3P water model (Jorgensen et al. 1983) is adopted to model water. Table 1 lists Van der Waals parameters for clay and water respectively determined by Katti et al. (2005). For the CHARMM force field, the total potential energy U_{tot} is expressed as a sum of the bonded energy U_{b} and the non-bonded energy U_{nb} , which is expressed as follows.

$$U_{nb} = \sum_{\text{van der Waals}} \sum_{i \neq j} 4\epsilon_{ij} \left[\left(\frac{\sigma_{ij}}{\gamma_{ij}} \right)^2 - \left(\frac{\sigma_{ij}}{\gamma_{ij}} \right)^6 \right] + \sum_{\text{electrostatic}} \sum_{i \neq i} \frac{q_i q_j}{\gamma_{ij}}$$

(1)

where r_{ij} is the distance between atom i and atom j, ϵ_{ij} and σ_{ij} are constants governing the Van der Waals energy (i.e., ϵ_{ij} is the well depth - energy and σ_{ij} is the distance between two atoms for the minimum energy (Frenkel & Smit 2002)), and q_i and q_j are the electrostatic charges on atom i and atom j, respectively. The parameters between two dissimilar atoms i and j are computed via $\epsilon_{ij} = \sqrt{\epsilon_i \epsilon_j}$ and $\sigma_{ij} = (\sigma_i + \sigma_j)/2$ (Frenkel & Smit 2002). Here (ϵ_i, σ_i) are parameters associated with atom i and (ϵ_j, σ_j) are parameters associated with atom j.

Table 1. Van der Waals parameters for clay and water (Katti et al. 2005).

Atom	ε_i	$\sigma_i(\text{Å})$	q _i
	(kcal/mol.Å)		
Al	0.150	6.30	1.68
Si	0.001	7.40	1.40
O(interior-1)	6.0	2.80	-0.96
O(interior-2)	6.0	2.80	-0.91
O(surface)	1.0	3.0	-0.70
H(clay)	0.0001	2.40	0.40
H(water)	0.046	0.44	0.417
O(water)	0.152	3.53	-0.834

Figure 2 shows the unsaturated clay-water model for the numerical simulation. In this model, two clay particles are placed parallel to each other with a gap (i.e., 42 Å for this study) between them. Each clay layer consists of 4 unit cells in the x-direction, 11 unit cells in the y-direction, and 1 unit cell in the z-direction. There are total 1760 atoms in each clay plate. The size of the water body in the x-y-z coordinate system is 21.12 Å x 40 Å x 40 Å, which includes 1183 water molecular or 3549 atoms. The total number of atoms of the model in this study is 7069. The size of the clay-water model in the x-y-z coordinate system is 21.12 Å x100.54 Å x 55.12 Å.

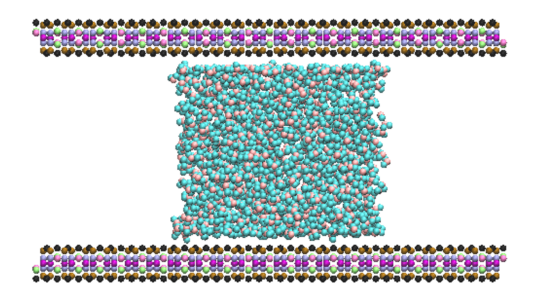


Figure 2. The clay-water model for the simulation.

3 SIMULATIONS

The MD simulation is conducted via LAMMPS (Plimpton 1995), a molecular dynamics simulator in which the CHARMm force fields for clay and water are supported. For the clay-water model, periodic boundary conditions are applied in all three directions (Frenkel & Smit 2002). The clay-water model is simulated under the plane strain condition at different elevated temperatures. In this study, the periodic cell size is four van del Waals cut-off distances (i.e., 10 Å) larger than the model size in the y and z directions to avoid any influence from the atoms in the neighboring cells. In the x-direction, to mimic the plane strain condition and continuation of the clay particles and the water body in the same direction, the width of the clay particle is exactly the same as the model size in the x-direction (i.e., 21.12 Å). The size of the simulation box in the x-y-z coordinate system is 21.12 Å x 140.54 Å x 90.12 Å.

The procedure known as the "Ewald sum" is adopted to calculate the long-range electrostatic forces accurately. A cut-off distance of 10 Å is used in this study as a sufficient distance truncating the van der Waals forces (Cygan et al. 2004). The MD simulations of the unsaturated clay-water system is conducted in the canonical ensemble (constant number of molecules, volume and temperature or NVT) at elevated temperatures. A time step of 0.025 fs (1 fs = 10^{-6} ns= 10^{-15} s) is used for all MD simulations. All simulations are run in parallel on 256 central processing units (CPUs) via HiPerGator – a supercomputer at the University of Florida. The focus of this study is on the impact of temperature on capillary forces.

3.1 *Monitoring the equilibrium state*

All variables fluctuate with respect to the simulation time in an MD simulation (Frenkel & Smit 2002). For this study, the time averages of the energy and temperature of the system are used to determine the equilibrium state of the unsaturated clay-water system. Figure 3 shows the variation of the system energy

with respect to the simulation time at temperatures of 318 K and 338 K, respectively.

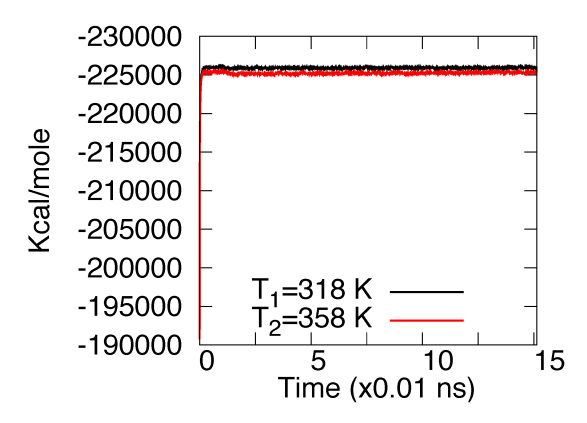
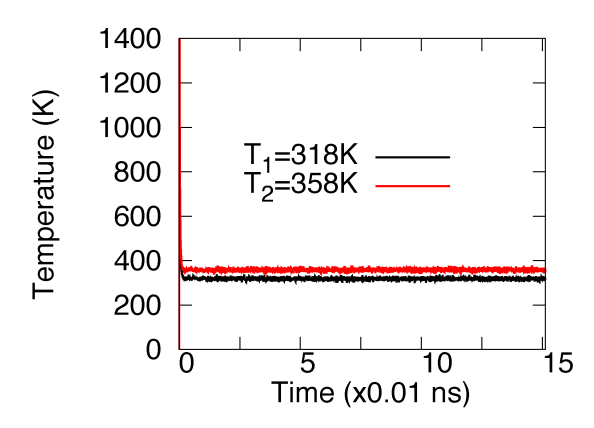


Figure 3. The variation of the system energy with respect to the simulation time at temperatures of 318 K and 358 K, respectively. Note: $1 \text{ ns} = 10^{-9} \text{ s}$.

The system energy jumps immediately at the beginning of the MD simulation. When the variation of the system energy repeats on a similar pattern, it suggests that the system has reached an equilibrium. The temperature of the system is controlled by a thermostat in LAMMPS (Plimpton 1995). To confirm the system under a steady state at the expected temperature, we also track the system temperature with the respect to the simulation time as shown in Figure 4 for two temperatures, 318 K and 358 K, respectively. Note that because of the scaling the temperature variation in Figs. 3 and 4 are not shown clearly.



Figures 4 The temperature variation of the clay-water system with respect to the simulation time.

From Figures 3 and 4, we observe that both the potential energy and the temperature of the system obtain a steady state at around 0.01 ns. It is noted that the simulation time on which the system obtains a steady state heavily depends on the computer capability (i.e. the number of CPUs and memory capacity) and the size of the numerical model (i.e. the number of total atoms).

4 RESULTS

In this section, we briefly present the preliminary results of the impact of temperature on capillary forces on clay particles imposed by a water meniscus between clay particles. We also report the topology of the water meniscus between clay particles at different temperatures.

4.1 Effect of temperature on capillary forces on clay particles

In this study, we present the impact of temperature on capillary forces at the atomic scale. The capillary force on the clay particle can be obtained directly from the MD simulation. Figures 5 shows the actual capillary forces on the top and bottom clay particles (refer to Figure 2) with respect to the simulation time at a system temperature of 318 K. Figure 6 shows the average capillary forces on the top and bottom clay particles with respect to the simulation time at a system temperature of 318 K. Comparison between Figure 3 and Figures 5 and 6 shows that the capillary force takes longer time to reach a steady state than the energy of the system needs.

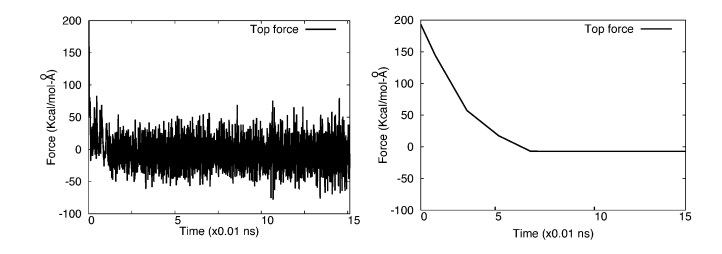


Figure 5. The variation of the actual capillary force (Left) and the average capillary force (Right) in the z-direction on the top clay particle with respect to the simulation time at temperature of 318 K.

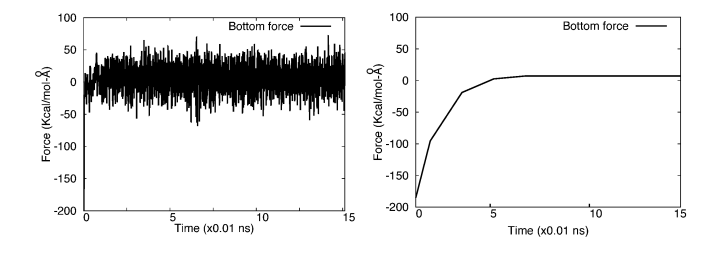


Figure 6. The variation of the actual capillary force (Left) and the average capillary force (Right) in the z-direction on the bottom clay particle with respect to the simulation time at temperature of 318 K.

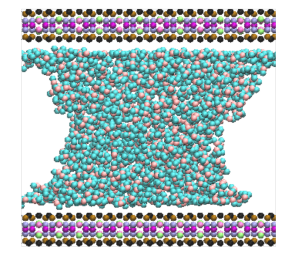
Table 2 summarizes the average capillary force in the z-direction on clay particles at three different temperatures directly obtained from the MD simulations. Table 2 shows that the increase of temperature of the system decreases the average capillary force imposed on the clay particle by the water meniscus.

Table 2. Capillary force in the z-direction on clay particles (Note: $1 \text{ Kcal/mol-} \text{Å} = 69.476 \times 10^{-12} \text{ N.}$)

_				
	Temperature	Capillary force (Kcal/mol-		Average
	of the clay-	Å) on clay particles in the z-		
	water sys-	direction		
	tem (Kelvin)	Тор	Bottom	
-	210	7 1 7	7 1 4	7 155
	318	7.17	7.14	7.133
	338	6.66	6.79	6.725
	358	6.32	6.69	6.505
-	water system (Kelvin) 318 338	direction Top 7.17 6.66	Bottom 7.14 6.79	o <u>-</u> e

4.2 Effect of temperature on the meniscus curvature

Figure 7 shows the final configuration of the water meniscus formed between two clay particles at temperature of 318 K and 358 K, respectively. From Figure 7, we observe that the topology of the water meniscus varies when the system temperature increases from 318 K to 358 K. For the preliminary study, we are not measuring the averaged contact angle and the water meniscus curvature directly from the MD simulations. However, we can observe from Figure 7 that the average contact between the clay particle and the water meniscus decreases when the system temperature increases.



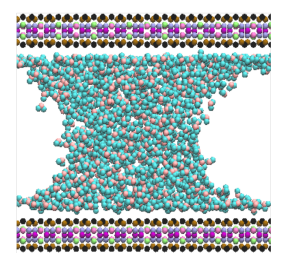


Figure 7. Final configurations of the water meniscus between clay particles at two temperatures, 318 K (Left) and 358 K (Right), respectively.

5 CONCLUSIONS

In this paper, we present a preliminary study on how temperature impacts the capillary force on clay particles imposed by a water meniscus between two parallel clay platelet particles via a full-scale molecular dynamics modeling. In this study, clay is modeled by a force potential for pyrophyllite (a 2:1 smectite mineral), and water is modeled by rigid TIP3P water model. All simulations are run through LAMMPS (a large-scale atomic/molecular massively parallel simulator) with 256 CPUs on a supercomputer. The preliminary results show that the increase of temperature will reduce the capillary forces on clay particles imposed by a water meniscus at the atomic scale. The numerical results also demonstrate that the contact angle between water meniscus and clay surface decreases with increasing temperature. The findings generated by full-scale MD simulations are consistent with the general trend that temperature increase decreases contact angle as shown by the published experimental data (Lu & Likos 2004). Further study is underway to measure the contact angle precisely via the computational topology at different system temperatures.

6 ACKNOWLEDGEMENTS

The study is supported by the National Science Foundation (CMMI1659932). The support is acknowledged.

7 REFERENCESS

- Amarasinghe, P. M., Anandarajah, A., & Ghosh, P. 2014. Molecular dynamic study of capillary forces on clay particles. *Applied Clay Science* 88:170-177.
- Brooks, B. R., Bruccoleri, R. E., Olafson, B. D., States, D. J., Swaminathan, S. A., & Karplus, M. 1983. CHARMM: a program for macromolecular energy, minimization, and dynamics calculations. *Journal of computational chemistry* 4(2), 187-217.
- Borja, R. I., Song, X., & Wu, W. 2013. Critical state plasticity. Part VII: Triggering a shear band in variably saturated porous media. *Computer Methods in Applied Mechanics and Engineering* 261, 66-82.
- Cygan, R. T., Liang, J. J., & Kalinichev, A. G. 2004. Molecular models of hydroxide, oxyhydroxide, and clay phases and the development of a general force field. *The Journal of Physical Chemistry B* 108(4), 1255-1266.
- Fredlund, D. G., & Rahardjo, H. 1993. Soil mechanics for unsaturated soils. John Wiley & Sons.
- Frenkel, D., & Smit, B. 2002. Understanding molecular simulations: from algorithms to applications. Academic Press.
- Jorgensen, W. L., Chandrasekhar, J., Madura, J. D., Impey, R. W., & Klein, M. L. 1983. Comparison of simple potential functions for simulating liquid water. *The Journal of chemical physics* 79(2), 926-935
- Katti, D. R., Schmidt, S. R., Ghosh, P., & Katti, K. S. 2005. Modeling the response of pyrophyllite interlayer to applied stress using steered molecular dynamics. *Clays and Clay Minerals* 53(2): 171-178.
- Lu, N., & Likos, W. J. 2004. Unsaturated soil mechanics. Wiley.
- Mitchell, J. K., & Soga, K. 2005. Fundamentals of soil behavior. John and Wiley.
- Ng, C. W., & Menzies, B. 2007. Advanced unsaturated soil mechanics and engineering. CRC Press.
- Plimpton, S., 1995. Fast parallel algorithms for short-range molecular dynamics. *Journal of Computational Physics* 117(1): 1-19.
- Skipper, N. T., Chang, F. R. C., & Sposito, G. 1995. Monte-Carlo simulation of interlayer molecular-structure in swelling clay-minerals. 1. Methodology. *Clays and Clay Minerals* 43(3): 285-293.
- Song X, & Borja RI. 2014. Mathematical framework for unsaturated flow in the finite deformation range. *International Journal for Numerical Methods in Engineering* 97(9):658–682.
- Song, X. 2017. Transient bifurcation condition of partially saturated porous media at finite strain. *International Journal*

- for Numerical and Analytical Methods in Geomechanics 41(1):135-156.
- Song, X., Wang, K., & Ye, M. 2018. Localized failure in un saturated soils under non-isothermal conditions. *Acta Geotechnica* 13(1), 73-85.
- Song, X, Ye, M., & Wang, K. 2017. Strain localization in a solid-water-air system with random heterogeneity via stabilized mixed finite elements. *International Journal for Numerical Methods in Engineering* 112, 1926–1950.
- Teppen, B. J., Rasmussen, K., Bertsch, P. M., Miller, D. M., & Schäfer, L. 1997. Molecular dynamics modeling of clay minerals. 1. Gibbsite, kaolinite, pyrophyllite, and beidellite. *The Journal of Physical Chemistry B* 101(9): 1579-1587.